Research Article

Xianchao Chen*, Jingchao Zhou, Ping Gao, Peijun Liu, and Qing Feng

Numerical simulation and optimization of biological nanocomposite system for enhanced oil recovery

https://doi.org/10.1515/ntrev-2024-0060
received March 19, 2024; accepted June 21, 2024

Abstract: Nanofluid flooding is a novel technology with potential for enhanced oil recovery. In this study, a biological nanocomposite system was formed by mixing hexamethyldisilazane-modified hydrophobic nano-SiO_2 with a biosurfactant produced by *Bacillus*. The stability of the system, its influence on rock wettability, and fluid interfacial tension were investigated experimentally. Numerical simulation methods were employed to simulate the displacement efficiency of the biological nanocomposite system and optimize the injection parameters. Finally, the application effects of the system in the field were evaluated. Results indicated that the biological nanocomposite system could change rock wettability and significantly reduce the interfacial tension to 1.8 mN/m at low concentrations. The core flooding results showed that the maximum oil recovery factor of the system reached 47.07%. Numerical simulations optimized the optimal injection concentration to be 7,000 ppm and the volume of injection to be 1.75×10^{-2} pore volumes, resulting in an oil increment exceeding 10,000 m^3 in field application. This study provides a solution for the green development of oil reservoirs and provides effective technical support for the numerical simulation and process scheme optimization of biological nanocomposite systems.

Keywords: biological nanocomposite system, numerical simulation model, parameter optimization

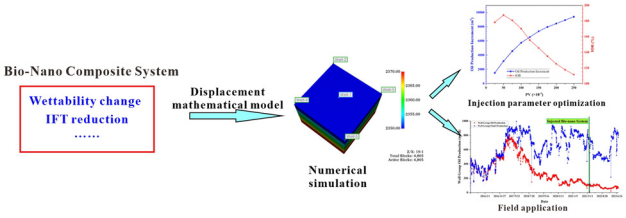

Graphical abstract

1 Introduction

With oil exploitation in recent decades, most of the old oil fields have entered the middle and late stages of development. After primary and secondary exploitation, nearly half of the oil reservoirs reserves remain undeveloped [1], despite the fact that chemical flooding methods such as surfactant flooding, polymer flooding, alkali flooding, and composite flooding have significantly improved the recovery rate of many old oil fields. However, because chemical flooding is more sensitive to oil field salinity and temperature, its practical application effect of chemical flooding is much smaller than its theoretical design effect [2]. The remaining newly discovered reservoirs exhibit significant seepage resistance, small pore structure, and poor pore connectivity, making development challenging and recovery rates low. Therefore, more innovative enhanced oil recovery (EOR) technology is required to increase oil field production.

Since the 1960s, when the famous physicist Richard Feynman first proposed the concept of nano, nanomaterials and nanotechnology have made great progress. Nanoscale (1–100 nm) materials, due to their small particle size, large specific surface area, and high surface energy, exhibit unique micro-physical and chemical properties that are different from other materials composed of the same chemical elements, such as electrical properties, magnetic properties, thermal properties, *etc.* By using these properties of nanomaterials, nanotechnology based on nanomaterials has been widely used in chemical, electronic information, biomedical,

*** Corresponding author: Xianchao Chen**, College of Energy, Chengdu University of Technology, Chengdu, 610059, China,
e-mail: chenxianchao2005@126.com, mangix2010@gmail.com
Jingchao Zhou, Peijun Liu: College of Energy, Chengdu University of Technology, Chengdu, 610059, China
Ping Gao: Chuanqing Drilling & Production Engineering Research Institute, Deyang, 618300, China
Qing Feng: China Oilfield Services Limited Oilfield Production Optimization Institution, Tianjin, 300459, China

and military industries [3,4]. Similarly, nano-materials have also been used in the field of improving oil recovery.

At present, nanoparticles used to improve oil recovery can be divided into four types: inorganic nanoparticles, carbon-based nanoparticles, organic nanoparticles, and composite nanoparticles. Nano-oil displacement technology is a technology that adds nanoparticles to the displacement fluid to improve the oil displacement effect. The corresponding nano-oil displacement agent can be divided into three types: nanofluids, nanoemulsions, and nano-assisted oil displacement [5]. For the mechanism of nanoparticle oil displacement, scholars have proposed a variety of explanations to discuss, but these explanations have not formed a unified theory. In general, the mechanism of nanoparticle EOR has the following points: altering rock wettability, reducing interfacial tension, structural separation pressure effect, and improving mobility ratio.

The wettability of reservoirs is one of the significant factors affecting the ultimate oil recovery rate, and the alteration of wettability in reservoir pore channels by nanoparticles has been confirmed in many laboratory experiments. Onyekonwu and Ogolo [6] investigated the ability of nanoparticles to change wettability and enhance recovery rates, finding that in hydrophilic core samples, neutral hydrophobic nanoparticles can improve the recovery rate at a concentration of 3,000 ppm, while hydrophilic nanoparticles, due to their enhancement of the core's hydrophilic properties, reduce the recovery rate. Tola *et al.* [7] studied the wettability changes in sandstone caused by zinc oxide nanoparticles formulated into nanofluids. The research indicates that nanofluids have the potential to transform wettability from hydrophobic to hydrophilic on oil films and oil-saturated sandstone surfaces. The adsorption of different nanoparticles in the reservoir also leads to varying changes in rock wettability. Li and Torsæter [8] and Li *et al.* [9] conducted a series of studies on the wettability alteration induced by nanoparticle adsorption. The experiments demonstrated that the adsorption of hydrophilic polysilicon nanomaterials within the pore throats is multilayered, while that of hydrophilic silica colloidal nanoparticles is monolayered. Subsequent research using visualization techniques investigated the impact of nanoparticle adsorption on wettability changes. Both two-dimensional (2D) and three-dimensional images revealed that during the injection of nanofluids, nanoparticles adhere to the surfaces of rock mineral particles, forming a water film during the oil displacement process. This water film prevents the mineral particle surfaces from being wetted by oil. Overall, the adsorption process of nanoparticles on rock minerals is central to wettability alteration, with electrostatic repulsion, non-electrostatic adhesion forces, and structural interactions driving the change in wettability [10].

Nanofluids can also affect the oil–water interfacial tension. The enhancement of oil recovery in reservoirs is primarily considered from two aspects: increasing the swept volume of the displacement system and improving the efficiency of oil washing. The magnitude of the oil–water interfacial tension influences the efficiency of oil washing. Nanoparticles, due to their small size and large specific surface area, possess certain interfacial activity and can adsorb at the oil–water interface, thereby reducing the oil/water interfacial tension [11]. Scholars have enhanced the performance of nanoparticles by chemically altering the hydrophilic or hydrophobic properties of their surfaces, enabling the nanoparticles to remain persistently stable at the oil–water interface. This action, similar to that of surfactants, reduces the molecular force differences at the interface, leading to a decrease in interfacial tension. Ultra-low oil–water interfacial tension can promote the mutual solubility of oil and water, forming emulsions [12], which improves the mobility of crude oil and ultimately enhances the efficiency of oil displacement.

The structural separation pressure effect is also one of the commonly discussed mechanisms for EOR, a theory first introduced by Wasan and Nikolov [13] and Wasan *et al.* [14]. Theoretical and experimental research indicates that due to the imbalance on solid surfaces, the oil contact angle is larger on hydrophilic surfaces. Under the influence of electrostatic repulsion and Brownian motion, nanoparticles in the fluid generate a pressure at the three-phase boundary of solid, water, and oil that resists the adhesion of the fluid to the solid surface, facilitating the separation of the fluid. The higher the concentration of nanoparticles, the stronger the force exerted [15], leading to the spontaneous formation of a wedge-shaped thin film structure. This structure generates a positive thrust that can strip oil and gas from the rock surface, thereby increasing the recovery rate [16]. Lim *et al.* [17] have shown through experiments that an increase in nanoparticle volume fraction, temperature, and rock hydrophilicity can also accelerate the rate at which the separation pressure strips the crude oil. This mechanism can be harnessed to develop new types of EOR nanomaterials. Wu *et al.* [18] have developed 2D flake-like nanomaterials that can create an osmotic pressure at the oil–water interface. Driven by the pressure of the liquid flow, the nanofluid can spread along the surface, causing the residual oil in the pores to detach.

In addition to experimental studies on the mechanisms of nanofluid-EOR, scholars have also conducted extensive numerical simulation research. Numerical simulation methods can be mainly categorized into three types: lattice Boltzmann

method simulations, molecular dynamics simulations, and computational fluid dynamics (CFD) simulations. CFD methods can further be subdivided into pore network models, interface tracking methods based on the Navier–Stokes (N–S) equations, and smoothed particle hydrodynamics [19,20]. Through these simulation methods, researchers have explored the mechanisms by which nanoparticles enhance recovery rates at the microscopic level [21–23]. At the macroscopic level, numerical simulations can evaluate the effectiveness of nanofluids in EOR. Esfe *et al.* [24] used finite-element numerical methods to study the impact of nanofluids on EOR in heterogeneous anticline reservoirs; Long *et al.* [25] investigated the effectiveness of nanofluid-assisted hydraulic fracturing through numerical simulations. Overall, although there are relatively comprehensive theoretical models for the adsorption, desorption, and convective diffusion of nanoparticles in porous media, numerical simulations of nanofluid-EOR at the field scale are still lacking, and related research has not yet optimized the process parameters of the displacement system, necessitating further supplementation.

In recent years, nanofluids have been applied to enhance oil recovery in major oil fields in China and achieved good results. In 2018, CNPC developed the first generation of nanofluid iNanoW1.0 and then conducted pilot tests in the ultra-low permeability reservoir of Changqing Oilfield, which showed the characteristics of increasing liquid and oil [26]. Yanchang Oilfield applied nanofluids to tight oil reservoirs, and the field test results showed that the average oil production of oil wells increased significantly [27]. In addition, Daqing Oilfield and Tahe Oilfield also used 2D nanomaterials for flooding field tests, achieving good results in reducing water cut and increasing oil production [28,29]. CNOOC's Penglai Oilfield used nanodispersion system for profile control, and the water cut of a single well decreased significantly, up to 17%, and the oil increase effect of well groups reached 6 400 m^3 [30]. In order to achieve green and efficient development of oil fields, CNOOC developed a biological nano-oil displacement agent system, which can change rock wettability to improve oil phase permeability, significantly reduce oil–water interface tension, and ultimately improve oil washing efficiency [31].

The combination of biogenic substances extracted from plants or microorganisms with nanoparticles has been demonstrated to have the potential to enhance oil recovery rates [32–34]. Nanoparticles can improve the efficiency of traditional oil displacement systems, while surfactants and polymers can enhance the stability of nanoparticles [35]. Biosurfactants are excellent carriers and dispersants for nanoparticles, and their synergistic effect possesses oil recovery functions such as wettability alteration, interfacial tension reduction, mobility control, and viscosity reduction [36]. Moreover, the composite system can maintain stability under high-temperature and high-salinity conditions [37]. In addition, compared to traditional EOR chemicals that may pose potential environmental hazards [38], the use of biomaterials to generate biosurfactants is also a low-cost, environmentally friendly, and efficient approach [39,40]. Similar to the EOR agents developed by CNOOC, this study utilizes a biological nanocomposite system composed of modified nanoparticles and biological-based dispersants. This system exhibits superior performance compared to traditional chemical EOR systems. However, there is a scarcity of research on field-scale numerical simulation methods for oil recovery using biological nanocomposite system, despite the existence of well-established models for nanoparticle transport and mass transfer and simulations of nanoparticle flow in larger-scale porous media, which have yet to reach the reservoir scale. Additionally, studies on the optimization of injection parameters are still lacking. This article investigates the performance of the biological nanocomposite system and its effects on the wettability of reservoir rocks and the interfacial tension of fluids through experimental research. Subsequently, a multiphase, multi-component model for oil recovery using the biological nanocomposite system is established and validated based on the experimental findings. Finally, optimization of injection parameters is conducted in terms of injection timing, injection volume, and injection concentration and applied to well groups. The study reveals the potential of the biological nanocomposite system to enhance oil recovery and supplements the optimization methods for related process parameters.

2 Performance evaluation experiment of biological nanocomposite system

2.1 Preparation of biological nanocomposite system

2.1.1 Materials

Analytical reagent hydrophobic nano-SiO_2, surface modified with hexamethyldisilazane, purchased from Shanghai Aladdin Biochemical Technology Co., LTD. (Shanghai, China). Lipopeptide biosurfactant, produced by the metabolism of *Bacillus* 3096-3, provided by China Oilfield Services Co., LTD.

2.1.2 Synthesis of biosurfactant

The laboratory uses *Bacillus* 3096-3 to produce lipopeptide surfactants. The experimental steps are as follows: 12.5 mL of *Bacillus* 3096-3 bacterial solution was added to 250 mL of embryonic stem cells medium and cultured in a shaking incubator at 37°C for 120 h, and then centrifuge was used to centrifuge the fermentation solution obtained, and the upper clear solution was taken as lipopeptide biosurfactant. Refer to the previous research for specific experimental procedures [31].

The modified nanoparticles and the lipopeptide biosurfactant solution were mixed in a certain proportion and stirred under ultrasonic conditions for 20 min until the solution was clear, and the biological nanocomposite system was prepared.

The biological nanocomposite system is primarily composed of modified nanoparticle and biological-based surfactants. The modified nanoparticles mainly contribute to the oil displacement, while the biological-based surfactants serve two purposes: first, they enhance the dispersion of the modified nanoparticles within the system, and second, they exhibit certain surfactant-like properties that can improve the oil recovery rate. After the injection of the biological nanocomposite system, the positively charged modified nanoparticles in the system readily adsorb onto the sandstone reservoir walls. During this adsorption process, a separation pressure is generated, which strips the oil adhering to the rock, leading to an increase in the crude oil recovery rate [41]. Following adsorption, the films formed by the nanoparticles can also reduce flow resistance and enhance the permeability of the reservoir [42,43] (Figure 1).

2.2 Dispersion of biological nanocomposite system

One of the significant challenges in the application of nanoparticles in oil reservoirs is that they tend to accumulate, which will block the seepage channel and reduce the recovery rate after injection into the formation. Therefore, the dispersion of nanoparticles applied in oil reservoirs is important.

Add 20 mL of biological nanocomposite system mother liquor to 180 mL of deionized water and stir at room temperature (25°C) at a rate of 300 rpm for 10 min. Then, withdraw 10 mL of the prepared biological nanocomposite system and measure the particle size and zeta potential of the nanoparticles within the system using dynamic light scattering. The measurement results are depicted in Figures 2 and 3.

From Figure 2, it can be observed that with the increase in stirring time, the particle size of the modified nanoparticles in the biological nanocomposite system first decreases and then increases, with an average particle size of 58.10 nm at a stirring time of 20 min. This is because the hydrophobic groups of the surfactants on the particle surface point towards the particle surface, while the polar groups point towards the aqueous phase, which is conducive to the dispersion of nanoparticles in water. Additionally, surfactants, especially bio-based surfactants, due to their unique spatial structure, form an adsorption layer on the particle surface that generates spatial potential energy, preventing particle-to-particle attraction and aggregation, resulting in a stable nanofluid solution.

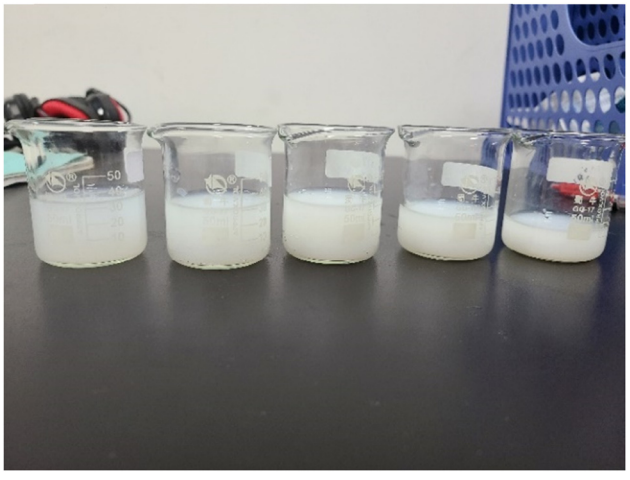

Figure 1: Biological nanocomposite systems with varying mass concentrations (from left to right, the mass concentrations are 0.1, 0.2, 0.3, 0.4, and 0.5 wt%, respectively).

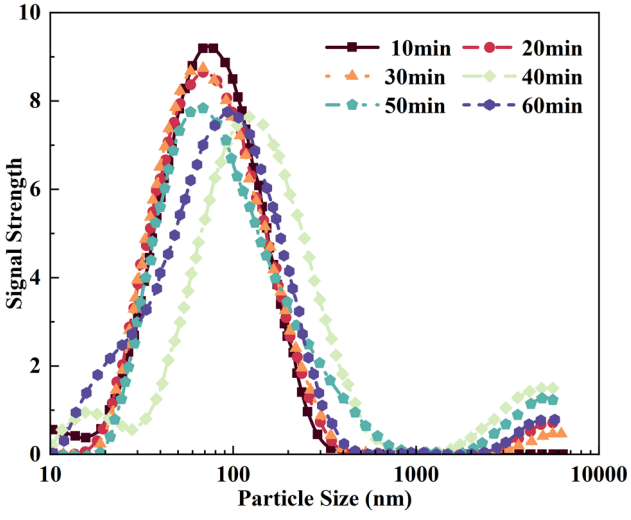

Figure 2: Particle size distribution of biological nanocomposite system at different stirring times.

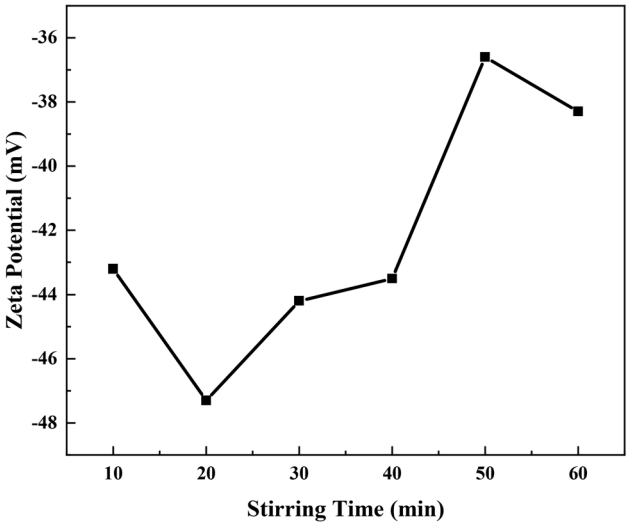

Figure 3: Changes of Zeta potential of biological nanocomposite system with stirring time.

The variation of the zeta potential curve of the nanofluid is due to the interaction between nanoparticles and the adsorption and redistribution of biosurfactant molecules on the surface of the particles. From Figure 3, it can be seen that the absolute values of the zeta potential of the biological nanocomposite system are all greater than 30 mV. When the zeta potential of the nanoparticles exceeds 30 mV, the electrostatic repulsion between the nanoparticles will be greater than the van der Waals forces, allowing for stable and uniform dispersion [44].

2.3 Effect of biological nanocomposite system on wettability

To investigate the impact of the biological nanocomposite system on the wettability of the reservoir, it is necessary to measure the wettability angles before and after the application of the biological nanocomposite system. To study the effects of the biological nanocomposite system on different lithologies of oil reservoirs, following the experimental protocols of previous researchers [45], calcite is used as an approximation for carbonate rocks, natural mineral quartz is used as an approximation for sandstone, and amorphous glass is employed as a control group. Subsequently, the wettability angles are measured using the sessile drop method (Figure 4).

Table 1 shows the wetting angle data of quartz, calcite, and glass in different mass concentrations of biological nanocomposite systems.

From Figure 5, it is evident that due to the use of minerals instead of actual core samples, the initial wettability angle exhibits a more ideal neutral wettability different from that of the actual oil reservoir. Subsequent measurements using the biological nanocomposite system reveal that the oil/displacing agent/mineral three-phase contact angle significantly decreases, and as the concentration increases, the reduction in the oil/displacing agent/mineral three-phase wettability angle becomes increasingly larger. This is also in line with the findings of previous research [45].

It can be observed that the biological nanocomposite system has a relatively minor impact at low concentrations (0.1, 0.2 wt%), with the reduction in the quartz wettability angle being very small, less than 10° (8.86° and 9.39°, respectively). However, the effect becomes significantly noticeable at 0.3% concentration, with a reduction value reaching 19.03°, and the wettability changes rapidly with increasing concentration, with the maximum reduction value reaching 34.7°. Although the wettability of calcite is altered, the reduction in the wettability angle is very small, with the maximum change value being only 6.25°. Glass, due to its inherently hydrophilic nature, shows a less pronounced effect of the biological nanocomposite system on wettability, with the maximum change in wettability angle being only 5.04°.

This is due to the fact that the surface of quartz minerals primarily carries a negative charge, making it

Figure 4: Photos of calcite and quartz before and after cutting.

Table 1: Three-phase wetting angles of different concentrations of biological nanocomposite systems and different minerals

	Concentration (wt%)	0	0.1	0.2	0.3	0.4	0.5
Quartz	Average wetting angle (°)	102.98	94.12	93.31	83.95	78.28	68.28
	Wetting angle reduction value (°)	—	8.86	9.67	19.03	24.70	34.70
	Reduction range (%)	—	8.60	9.39	18.48	23.99	33.70
Calcite	Average wetting angle (°)	99.28	95.37	95.05	93.8	94.11	93.03
	Wetting angle reduction value (°)	—	3.91	4.23	5.48	5.17	6.25
	Reduction range (%)	—	3.94	4.26	5.52	5.21	6.30
Glass	Average wetting angle (°)	44.51	42.77	40.44	40.07	39.40	39.47
	Wetting angle reduction value (°)	—	1.74	4.07	4.44	5.11	5.04
	Reduction range (%)	—	3.91	9.14	9.98	11.48	11.32

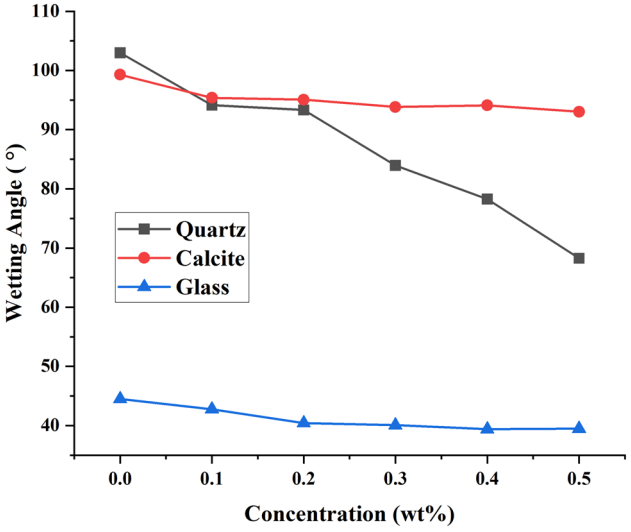

Figure 5: Three-phase wetting angles of different concentrations of biological nanocomposite systems with different minerals and oils.

more susceptible to the adsorption of positively charged modified nanoparticles, which results in a very noticeable change in the wettability angle of quartz. Conversely, the surface of calcite minerals mainly carries a positive charge, making it difficult for the modified nanoparticles to adsorb onto the calcite, leading to a smaller change in the wettability angle observed in the experiments [46,47].

Within the reservoir, when nanoparticles adsorb onto the rock wall surfaces, they generate a separation pressure that strips the crude oil from the rock wall, a process also known as the wedge-shaped squeezing mechanism for enhancing oil recovery; the nanoparticle film formed after adsorption on the rock wall also serves to reduce flow resistance [43]. Simultaneously, the surfaces of quartz and silicate minerals in sandstone reservoirs predominantly exhibit negative charges, while the mineral surfaces in carbonate reservoirs mainly carry positive charges [46,47]. Therefore, under general conditions, the biological nanocomposite system is expected to improve wettability more effectively in sandstone reservoirs than in carbonate reservoirs; in carbonate reservoirs, if the goal is to change wettability by adsorbing nanoparticles onto the rock wall after injection, the nanoparticles should ideally carry a negative charge or be uncharged.

2.4 Effect of biological nanocomposite system on interfacial tension

The extent of EOR in a reservoir is primarily determined by two factors: the swept volume of the injected water or displacing agent and the efficiency of oil washing. The magnitude of the oil–water interfacial tension affects the efficiency of oil washing. Conventional surfactants mainly improve the recovery rate of crude oil by reducing the interfacial tension. Surfactant molecules possess both hydrophilic and lipophilic groups, which give them amphiphilic properties, allowing them to dissolve in the phase with similar polarity at the oil–water interface, reducing the polarity difference and thus lowering the interfacial tension [48]. In the biological nanocomposite system, both the modified nanoparticles and surfactants contain amphoteric groups, which can be observed to rapidly decrease the oil–water interfacial tension after the addition of the system. Figure 6 illustrates the oil–water interfacial tension of biological nanocomposite systems with different mass concentrations.

At a concentration of 0.1 wt%, the interfacial tension can be reduced to 1.8 mN/m, indicating that the biological nanocomposite system is capable of significantly reducing the oil–water interfacial tension even at low concentrations. Furthermore, at a concentration of 0.5 wt%, the biological nanocomposite system can further reduce the oil–water interfacial tension to the order of 10^{-3}.

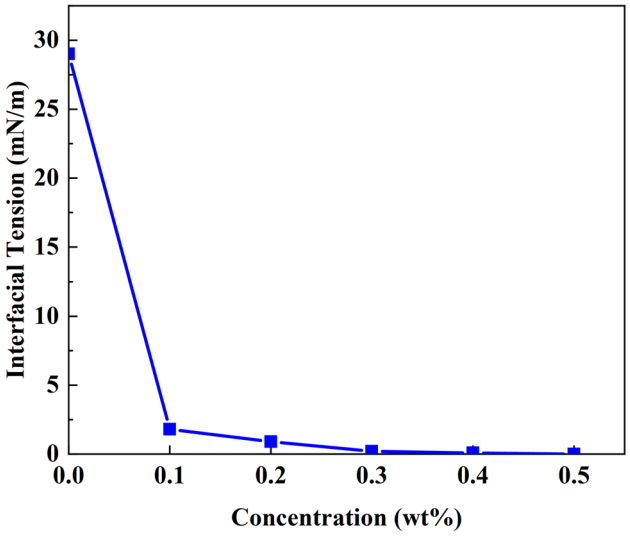

Figure 6: Effect of biological nanocomposite system on oil–water interfacial tension [41].

Therefore, it can be concluded that as the concentration of the biological nanocomposite system increases, the oil–water interfacial tension rapidly decreases, and ultra-low oil–water interfacial tension can promote the mutual solubility of oil and water, forming an emulsion [12]. This characteristic significantly enhances the oil displacement performance of the biological nanocomposite system, enabling the displacement of crude oil that was previously difficult to mobilize, thereby increasing the oil recovery rate of the reservoir.

In fact, the majority of current strategies for enhancing crude oil recovery focus on improving the fluid mobility within the formation and the wettability of the oil/water/rock three-phase system [49]. The biological nanocomposite system can effectively improve the wettability angles of the oil/water/rock three-phase system. The separation pressure enables the effective detachment of crude oil from the rock wall surfaces, enhancing the oil recovery rate. Additionally, the reduction in interfacial tension also leads to the formation of a certain amount of Pickering emulsion, which improves the mobility of the crude oil and thus increases the recovery rate.

3 Mathematical model of biological nanocomposite system displacement

The multiphase and multi-component coupling model of biological nanocomposite system is mainly composed of the following four parts: 1) seepage model of water drive reservoir, 2) modified nanoparticle adsorption and transport model, 3) dynamic porosity and permeability model, and 4) reservoir relative permeability change model.

3.1 Model assumptions

The seepage equation of oil–water–gas components in the water drive reservoir is the same as that of the black oil model, and its assumptions are as follows:

1) The percolation in the reservoir is isothermal and does not consider the temperature change of the reservoir.
2) There are three phase fluids of oil, gas, and water in the formation, and the flow of each phase fluid obeys Darcy's law.
3) Mass exchange occurs in the oil–gas phase and water–gas phase in the gas group.
4) The phase balance is completed instantaneously; that is, the time required for phase balance is not considered.
5) The water component exists only in the water phase, and there is no mass exchange between the oil and gas phase.
6) The rock reservoir is slightly compressible and anisotropic.
7) The fluid in the reservoir is compressible, and gravity and capillary forces have an effect on the percolation process.

For the black oil model, the continuity equations of the oil phase, water phase, and gas phase are, respectively,

$$\nabla\cdot\left[\frac{KK_{\mathrm{ro}}}{\mu_{\mathrm{o}}B_{\mathrm{o}}}(\nabla P_{\mathrm{o}}-\gamma_{\mathrm{og}}\nabla D)\right]+q_{\mathrm{o}}=\frac{\partial}{\partial t}\left[\frac{\phi S_{\mathrm{o}}}{B_{\mathrm{o}}}\right], \tag{1}$$

$$\nabla\cdot\left[\frac{KK_{\mathrm{rw}}}{\mu_{\mathrm{w}}B_{\mathrm{w}}}(\nabla P_{\mathrm{w}}-\gamma_{\mathrm{w}}\nabla D)\right]+q_{\mathrm{w}}=\frac{\partial}{\partial t}\left[\frac{\phi S_{\mathrm{w}}}{B_{\mathrm{w}}}\right], \tag{2}$$

$$\nabla\cdot\left[R_{\mathrm{s}}\frac{KK_{\mathrm{ro}}}{\mu_{\mathrm{o}}B_{\mathrm{o}}}(\nabla P_{\mathrm{o}}-\gamma_{\mathrm{og}}\nabla D)+\frac{KK_{\mathrm{rg}}}{\mu_{\mathrm{g}}B_{\mathrm{g}}}(\nabla P_{\mathrm{g}}-\gamma_{\mathrm{g}}\nabla D)\right]+R_{\mathrm{s}}q_{\mathrm{o}}+q_{\mathrm{g}}=\frac{\partial}{\partial t}\left[\frac{\phi S_{\mathrm{o}}R_{\mathrm{s}}}{B_{\mathrm{o}}}+\frac{\phi S_{\mathrm{g}}}{B_{\mathrm{g}}}\right]. \tag{3}$$

3.2 Continuity equation

In the composite system, the modified nanoparticles are considered as a component dissolved in the aqueous phase. According to the principle of mass conservation, the continuity equation can be written as

$$\nabla\cdot\left[c_{\mathrm{np}}\frac{KK_{\mathrm{rw}}}{\mu_{\mathrm{w}}B_{\mathrm{w}}}\nabla\left(\frac{\partial P_{\mathrm{w}}}{\partial x}-\gamma_{\mathrm{w}}\frac{\partial D}{\partial x}\right)\right]+\nabla\cdot[d_{\mathrm{p}}\phi S_{\mathrm{w}}\nabla c_{\mathrm{np}}]+q_{\mathrm{w}}c_{\mathrm{np}} = \frac{\partial(\phi S_{\mathrm{w}}c_{\mathrm{np}})}{\partial t}+\frac{\partial[F_{\mathrm{np}}\rho_{\mathrm{R}}(1-\phi)\hat{c}_{\mathrm{np}}]}{\partial t}, \tag{4}$$

where c_{np} is the concentration of modified nanoparticles, P is the formation pressure, and x is the distance from the injection hole bottom. S_{w} is the water saturation, q_{w} is the water injection quantity, and d_{np} is the diffusion coefficient of modified nanoparticles. F_{np} is the percentage of the pore surface in contact with water.

3.2.1 Dynamic porosity and permeability model

The deposition and adsorption of modified nanoparticles in pores can lead to changes in the absolute permeability and porosity of reservoirs [50,51]

$$\phi=(\phi_0-\sum\Delta\phi), \tag{5}$$

where ϕ_0 is the initial porosity, $\sum\Delta\phi$ represents the change of porosity caused by adsorption and desorption of modified nanoparticles in the porous media of the reservoir

$$K=K_0[(1-f)k_{\mathrm{f}}+f\phi/\phi_0]^n. \tag{6}$$

where K_0 is the initial absolute permeability of the reservoir. n is a constant, and the value can range from 2.5 to 3.5, and the general value is 3 [52]. k_{f} is the fluid flow coefficient of plugging pores. f is the flow efficiency coefficient, which can be obtained by the following formula:

$$f=1-\alpha V^*, \tag{7}$$

where α is the rate constant of adsorption of modified nanoparticles in oil phase to reservoir and V^* is the volume of modified nanoparticles that can be trapped by porous media per unit volume.

The adsorption of nanoparticles uses the Langmuir isothermal adsorption formula:

$$\hat{c}_{\mathrm{np}}=\frac{Ac_{\mathrm{np}}}{1+Bc_{\mathrm{np}}}, \tag{8}$$

where A and B are Langmuir constant.

3.2.2 Reservoir relative permeability model

For the relative permeability of the reservoir, the actual relative permeability is used before adding the modified nanoparticles. After adding the modified nanoparticles, the calculation was performed using the modified Brooks–Corey model [53]:

$$K_{\mathrm{rjc}}=K_{\mathrm{rjc}}^{\circ}\ S_{\mathrm{jR}}^{E_j}, \tag{9}$$

$$S_{\mathrm{jR}}=\frac{S_{\mathrm{j}}-S_{\mathrm{rjc}}}{1-S_{\mathrm{rwc}}-S_{\mathrm{roc}}}, \tag{10}$$

where j represents different phases (oil or water), K_{rjc} is the relative permeability of the j phase (oil or water), and K_{rjc}° is the maximum relative permeability of the j phase (oil or water). S_{jR} is the normalized saturation of the j phase (oil or water) and E_{j} is the Corey index of relative permeability and water saturation of the j phase (oil or water) in the presence of surfactant. S_{rwc} is the primary water saturation in the presence of surfactant. S_{roc} is the residual oil saturation in the presence of a surfactant.

After the addition of modified nanoparticles, since the relative permeability is largely related to the oil–water interfacial tension and is a function of the oil–water interfacial tension, the size of S_{rwc} and S_{roc} is affected by the interfacial tension. Refer to UTCHEM software for similar scaling methods for the treatment of surfactants [54–56], S_{rwc} and S_{roc} are expressed as follows:

$$\begin{cases}S_{\mathrm{rjc}}=0, & (\sigma<0.005\ \mathrm{mN/m})\\ S_{\mathrm{rjc}}=S_{\mathrm{rj}}\times\left(1+\dfrac{\lg\sigma}{2.3}\right), & (0.005\ \mathrm{mN/m}<\sigma<1\ \mathrm{mN/m})\\ S_{\mathrm{rjc}}=S_{\mathrm{rj}}, & (\sigma>1\ \mathrm{mN/m}),\end{cases} \tag{11}$$

where S_{rjc} represents the residual saturation of the j phase (oil or water) at the beginning of the nanoparticle injection and σ is the interfacial tension.

The endpoint relative permeability $K_{\mathrm{ric}}^{\mathrm{o}}$ and Corey index E_{i} are modified as functions of interfacial tension, so that the relative permeability curve at ultra-low interfacial tension shows a diagonal line in the relative permeation-water saturation plot

$$K_{\mathrm{ric}}^{\circ}=K_{\mathrm{ri}}^{\circ}+(1-K_{\mathrm{ri}}^{\circ})(S_{\mathrm{ri}}-S_{\mathrm{ric}}), \tag{12}$$

$$\begin{cases}E_{\mathrm{i}}=1, & (\sigma<0.005\ \mathrm{mN/m})\\ E_{\mathrm{i}}=n_{\mathrm{i}}+(1-n_{\mathrm{i}})(S_{\mathrm{ri}}-S_{\mathrm{ric}}),\\ (0.005\ \mathrm{mN/m}<\sigma<1\ \mathrm{mN/m})\\ E_{\mathrm{i}}=n_{\mathrm{i}},\ S_{\mathrm{ric}}=S_{\mathrm{ri}}, & (\sigma>1\ \mathrm{mN/m}),\end{cases} \tag{13}$$

where S_{ri} is the residual saturation of phase i (oil or water) at the end of water flooding under the oil–water interfacial tension of ordinary water injection and K_{ri}° is the endpoint relative permeability of phase i (oil or water) at the end of water flooding under the oil–water interfacial tension of ordinary water injection. n_{i} is the Corey index of phase i (oil or water) at the end of water flooding under the oil–water interfacial tension of ordinary water injection.

3.2.3 Boundary conditions

Equations (14)–(16) are the auxiliary equations of the coupling model of the biological nanocomposite system. Including the relationship between saturation and capillary force, pressure-volume-temperature physical properties equation:

$$S_o + S_w + S_g = 1, \tag{14}$$

$$p_{cow} = p_o - p_w, \tag{15}$$

$$p_{cgo} = p_g - p_o, \tag{16}$$

where S_o is the oil saturation, S_g is the gas saturation, p_o is the capillary pressure of the oil, p_w is the capillary pressure of water, and p_g is the capillary pressure of a gas.

The initial condition equation of the model is

$$p(x, y, z, t)|_{t=0} = p^0(x, y, z), \tag{17}$$

$$s_w(x, y, z, t)|_{t=0} = s_w^0(x, y, z), \tag{18}$$

$$s_o(x, y, z, t)|_{t=0} = s_o^0(x, y, z). \tag{19}$$

For the closed boundary of the reservoir, with the following boundary conditions:

$$\left.\frac{\partial p}{\partial n}\right|_L = 0. \tag{20}$$

Finally, the production control equation of the well is added to the reservoir:

$$Q_v(x, y, z, t) = Q_v(t)\delta(x, y, z), \tag{21}$$

$$p_{wf}(x, y, z, t) = p_{wf}(t)\delta(x, y, z). \tag{22}$$

where Q_v is the oil well production, p_{wf} is the bottom hole pressure, and $\delta_{(x,\ y,\ z)}$ is a Dirichlet function, if (x, y, z) corresponds to the well coordinates, $\delta_{(x,\ y,\ z)} = 1$, otherwise $\delta_{(x,\ y,\ z)} = 0$. That is, the change of water in the reservoir other than the well is ignored.

3.3 Model validation

The accuracy of the model is verified by core experiments. The injected PV of the selected core and biological nanocomposite system is shown in Table 2. The natural core was extracted from the oil field, which can reflect the actual reservoir conditions and make the experimental results more accurate and reliable than the artificial core. The experimental device is shown in Figure 7.

The numerical model was solved through the STARS simulator built by CMG software. The numerical model of the core was established with a total of 40 grids, the grids

Table 2: Experimental basic data

Parameters	Rock type	Porosity (%)	Permeability (mD)	Injection rate (mL/min)	Confining pressure (MPa)	Total injected PV
Value	Natural sandstone	20.14	176	0.1	10	0.1568

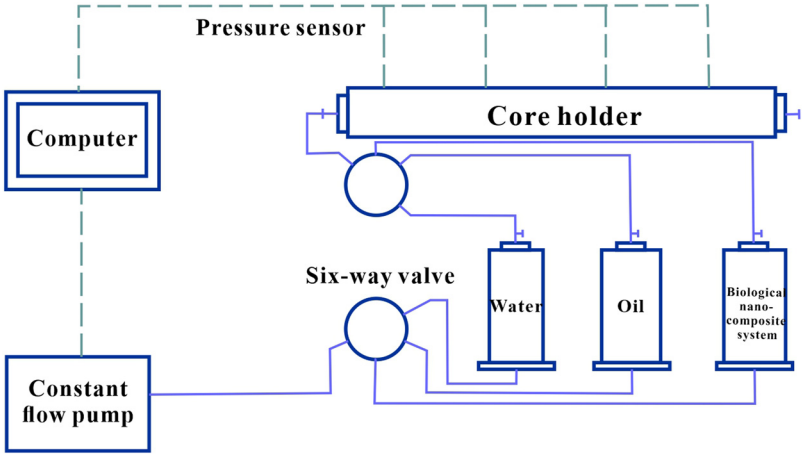

Figure 7: Flow chart of oil displacement experimental device of biological nanocomposite system.

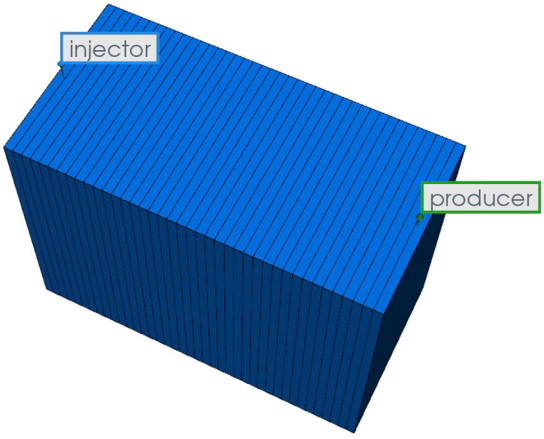

Figure 8: Core grid used for model validation.

are shown in Figure 8, and the results are shown in Figure 9.

Figure 9 shows the results of the core oil displacement experiment of the biological nanocomposite system and the model established in this article. As can be seen from the figure, in the stage of water flooding, the water cut and recovery degree start to rise rapidly at the 5th minute of injection, and the water cut reaches 95.03% and the recovery degree is 34.06% at the 14th minute; then, with the change of injection amount, the rising rate of water cut and recovery degree starts to slow down, and the water cut reaches the maximum of 99.35% at the 18th minute, and the recovery degree is 34.99% at this time.

The injection of the biological nanocomposite system began when the water cut exceeded 99%, and the water cut rapidly decreased to 95.71%, and the lowest water cut could be reduced to 93.19% with the increase of the injection

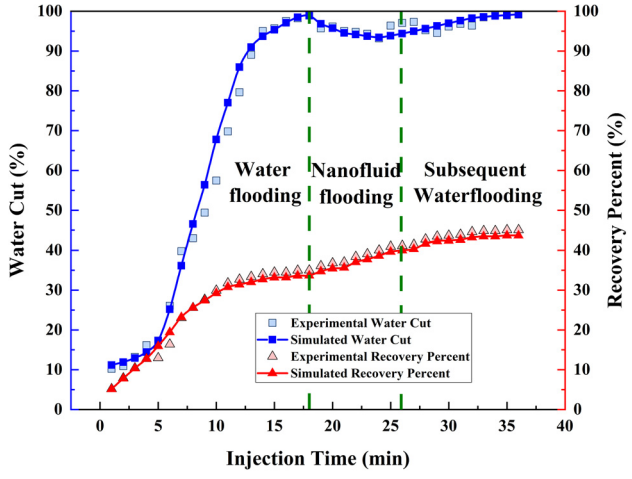

Figure 9: Comparison between simulated calculated values and actual experiments.

amount of the biological nanocomposite system; at the same time, after the injection of the biological nanocomposite system, the recovery degree also increased rapidly compared with the first water flooding, and with the increase of the injection amount of biological nanocomposite system, the recovery degree increased significantly in the 21st minute, because after a period of injection, the biological nanocomposite system and the oil in the core began to form emulsion, which increased the oil production rate, until the recovery degree reached 41.15% when the injection of biological nanocomposite system was stopped; in the process of injection of biological nanocomposite system, there was no obvious accumulation of nanoparticles in the produced liquid, and the injection pressure did not increase significantly, indicating that the injection of biological nanocomposite system was good.

In the subsequent water flooding stage, the recovery rate within 26–29 min is still faster than that in the late stage of the first water flooding, indicating that the biological nanocomposite system is still playing a role at this time. After that, the biological nanocomposite system flows out of the core with the increase in injection time, and the water cut begins to rise again. After a period of displacement, the recovery rate basically stops rising to 47.07%. From the core oil displacement experiment, it can be seen that the recovery rate can be increased from 34.99% to 47.07% with only 0.1568PV injected into the biological nanocomposite system, with an increase of 12.08%. Compared with other nanoparticles injected with half of the PV, it can get almost the same oil increase effect, with huge application potential [48]. At the same time, through the comparison with the experimental results, it can be found that the results obtained by using the numerical simulation model established in this paper are very close to the experimental value, so the model established in this article has high accuracy and can be used for subsequent research.

4 Optimization and application of numerical simulation model

Taking the basic rock data of the KL well group in Bohai Oilfield as an example, a conceptual model of the biological nanocomposite system for oil recovery was established using CMG reservoir numerical simulation software, as shown in Figure 10. The main parameters are as follows:

The reservoir thickness is 25 m, and the porosity and permeability settings of each layer are shown in Table 3.

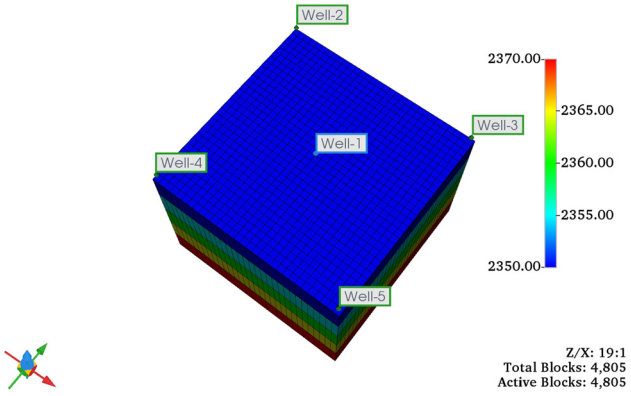

Figure 10: Conceptual model of biological nanocomposite system for oil recovery.

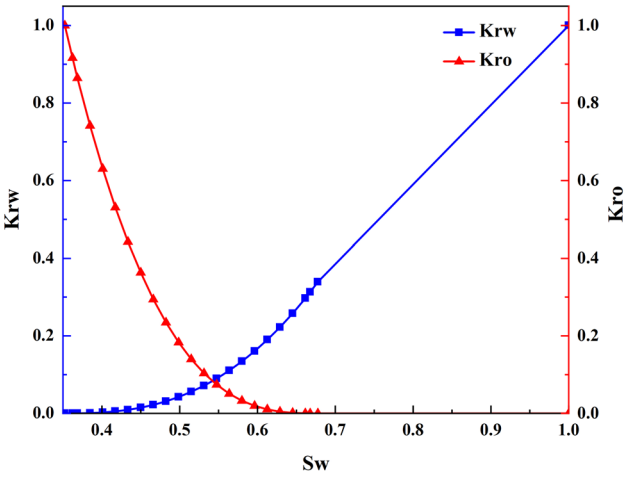

Figure 11: The relative permeability curves without biological nanocomposite system.

The layout of injection and production wells adopts a five-point well network, and the distance between injection and production wells is set at 434 m.

The maximum liquid production capacity of a single production well is set to 150 m^3/d, and the maximum injection rate of an injection well is set to 600 m^3/d.

The physical properties of crude oil are set based on actual formation data, with an initial formation pressure of 24 MPa.

The depth of the formation is 2,350 m, and the temperature is set at 75°C. Finally, the model has a mesh size of 31 × 31 × 5 = 4,805.

For the modification of wettability and interfacial tension between oil and water in the biological nanocomposite system, the Corey permeation model from equations (11)–(13) was used for interpolation characterization based on Figures 11 and 12.

4.1 Optimization of injection timing

The injection timing refers to the time node at which the reagent is injected. For chemical flooding, injection timing generally refers to the timing of injecting the chemical agent at different water content stages, which is generally measured by the water content value. Therefore, the injection timing of the biological nanocomposite system is determined by referring to the chemical flooding method and also based on the water content. At the same time, the actual injection time of the biological nanocomposite system in the oilfield is currently in the middle and later stages of oilfield development. At this time, the water content of the produced liquid is very high. Therefore, different injection times are set with water content of 79, 80.5, 82, 83.5, 85, 86.5, 88, 89.5, 91, and 92.5%, respectively.

From the analysis of the relationship between oil increment and injection timing in Figure 13, it can be seen that as the injection timing is delayed, the oil increment continuously decreases, which is basically consistent

Table 3: Conceptual model porosity and permeability of each layer

	Porosity (%)	Horizontal permeability (mD)	Vertical permeability (mD)
Layer 1	24.04	386	38.6
Layer 2	23.37	330	33.0
Layer 3	22.64	275	27.5
Layer 4	20.22	178	17.8
Layer 5	19.07	138	13.8

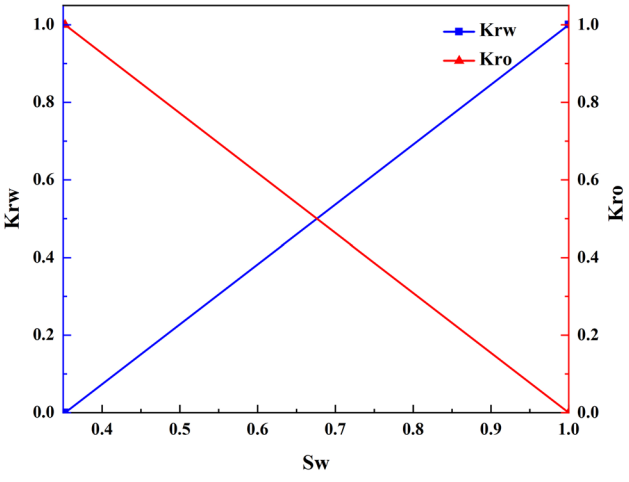

Figure 12: The relative permeability curves with biological nanocomposite system.

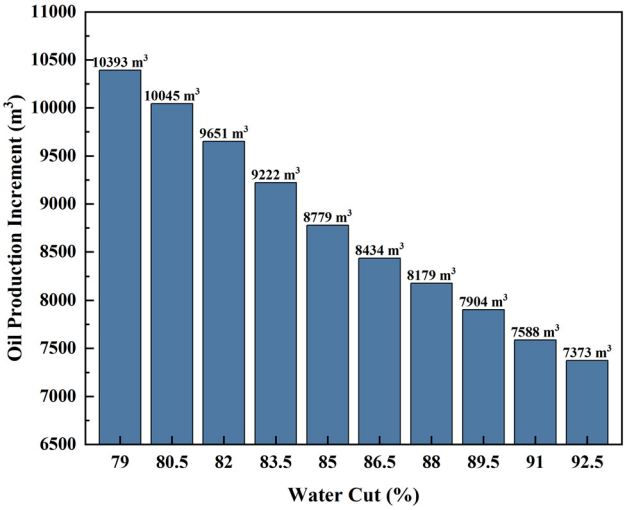

Figure 13: Relationship between oil increment and injection timing in the biological nanocomposite system.

with the general law of conventional chemical flooding. The maximum oil increase occurs in the early stage of injection and then decreases with the delay of injection time. This is because as the water content increases, the amount of crude oil in the formation decreases, and the amount of crude oil affected by the injection of the biological nanocomposite system is also less. In addition, some layers in the formation have formed advantageous flow channels, and it is difficult to drive the remaining oil by injecting the biological nanocomposite system at this time. This is different from the research results of some predecessors on the timing of nanoparticle injection [48]. On the one hand, it is because different types of nanoparticles are used, and on the other hand, the length of the core is limited in experiments at the core scale. Although nanoparticles also have the effect of increasing oil when the water content is low, they will continue to flow out at the outlet, causing a smaller proportion of nanoparticles that are difficult to drive remaining oil. However, as the water content increases, there are relatively more nanoparticles that are difficult to drive remaining oil, and the oil-increasing effect of nanoparticles is also better. Therefore, the final experimental results are different from the numerical simulation results.

4.2 Optimization of injection pore volume (PV)

For injection volume, injection PV multiple is generally used to measure it. As it is a conceptual model, it is set as the injection PV multiple of the entire reservoir. In the actual injection process, due to the cost of preparing nanoparticles, the injection amount is not large, so the injection PV number is set to 2.5×10^{-3}, 5.0×10^{-3}, 7.5×10^{-3}, 10.0×10^{-3}, 12.5×10^{-3}, 15.0×10^{-3}, 17.5×10^{-3}, 20.0×10^{-3}, 22.5×10^{-3}, 25.0×10^{-3} represents the injection amount of different biological nanocomposite systems. At the same time, the injection amount of biological nanocomposite systems needs to be considered not only from the perspective of oil increase, but also from the perspective of economic benefits. Therefore, the input–output ratio (IOR) index is used to analyze the economic benefits, which is defined as

$$\text{Output input ratio} = \frac{\text{Crude oil revenue}}{\text{Input costs}}, \tag{23}$$

In the formula, the input cost only includes the material cost of the biological nanocomposite system, while the exchange rate ignores exchange rate fluctuations and is uniformly set to 6.8 US dollars and Chinese yuan. The economic benefits of output only consider the economic value of oil increase, without considering the fluctuation of crude oil prices. The data are based on the west texas intermediate crude oil futures prices on trading days from January 2, 2020, to December 30, 2023 (with an average price of $69.97 per barrel), which is generally $70 per barrel. Due to the high cost of offshore operations, oilfield sites generally require an IOR greater than 120% before the plan can be implemented. Figure 14 shows the increase in oil production and the change in IOR under the injection of biological nanocomposite systems with different PV multiples.

From the analysis of the relationship between the oil increment and the number of injected PV in Figure 14, it can be seen that within a certain range, as the number of injected PV increases, the oil increment continuously increases, and the increase is very large. But after the increase in the

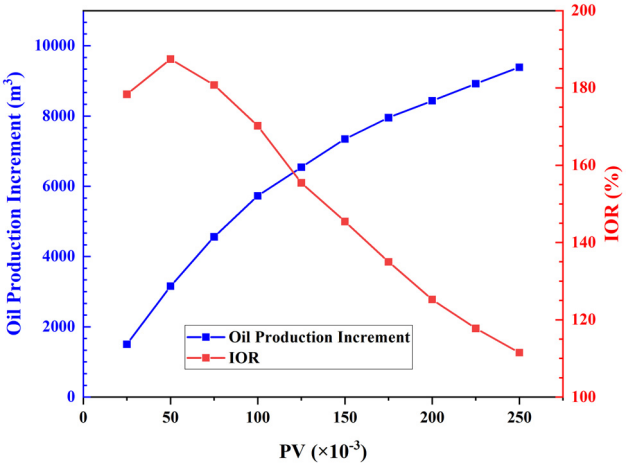

Figure 14: Oil increment and IOR under different injection PVs.

number of injected PV reaches a certain value, although the increase in the number of injected PV will lead to an increase in oil production, the increase is smaller compared to the increase when injecting small doses of biological nanocomposite systems. This is because after the injection amount reaches a certain level, the amount of modified nanoparticles that can be adsorbed on the rock has reached its limit and cannot be further adsorbed, making the wettability of the rock reservoir more hydrophilic. At the same time, although the dispersion of the biological nanocomposite system is very well, due to the high concentration, the modified nanoparticles adsorb in the reservoir, causing the flow channel to be blocked to a certain extent, resulting in a decrease in the increase in oil production. However, due to the excellent dispersion, the aggregated modified nanoparticles quickly disperse into the aqueous phase, so there is still a trend of an increase in oil production. Further analysis of the IOR reveals that as PV increases, the IOR shows a trend of first increasing and then decreasing. Taking into account this, an injection PV of 1.75×10^{-2} can be chosen as the optimal injection amount.

4.3 Optimization of injection concentration

For injection concentrations, set the injection concentrations to 1,000, 2,000, 3,000, 4,000, 5,000, 6,000, 7,000, 8,000, 9,000, and 10,000 ppm for different biological nanocomposite systems.

Figure 15 shows the increase in oil production and the change in input–output ratio under the injection of different concentrations of biological nanocomposite systems.

From the analysis of the relationship between oil increment and injection concentration in Figure 15, it can be seen that injecting the biological nanocomposite system can effectively increase oil, but the oil increase effect is not significant at low concentrations. Subsequently, as the injection concentration increases, the oil increment increases rapidly. However, although the oil increment still increases after the injection concentration reaches a certain value, the increase amplitude will slow down. This is because there is an upper limit to the adsorption of modified nanoparticles in the rock reservoir and displacement front, and excessively high concentrations of modified nanoparticles may actually block the pores, preventing a significant increase in oil production. From the relationship between IOR and injection concentration, it can be seen that as the concentration increases, the IOR first increases rapidly and then shows a decreasing trend. Except for 1,000 ppm, the IOR is greater than 100%, indicating a very good IOR; At 5,000 ppm, there is the highest IOR, but at this time, the oil increment is only 7259.9 m^3. In the actual extraction process, it is also necessary to consider the factor of maximizing the exploitation and utilization of crude oil resources. After 5,000 ppm, for every 1,000 ppm increase in concentration, the increase in oil production is 692.0, 624.6, 486.6, 422.0, and 375.0 m^3, respectively. Therefore, 7,000 ppm can be optimized as the optimal injection concentration.

In summary, the earlier the injection of the biological nanocomposite system, the better the effect. At the same time, the more the injection amount of the biological nanocomposite system, the better the oil enhancement effect, but the change in oil enhancement amount with the increase of injection amount becomes smaller and smaller. Considering the economic value, it can be determined that 17.5×10^{-3} is the optimal injection amount. The injection concentration and injection amount have a similar pattern, and 7,000 ppm can be selected as the optimal injection concentration.

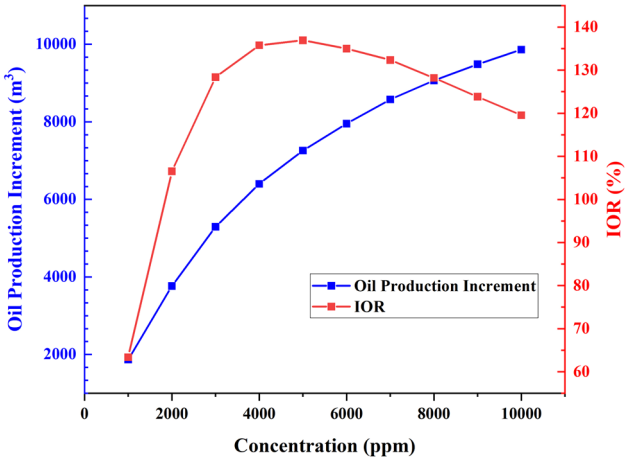

Figure 15: Oil increment and IOR under different injection concentrations.

4.4 Field application

Based on the optimization results of injection parameters, the implementation of biological nanocomposite oil displacement technology applied to actual well groups. The B1 block of Bohai K1 oilfield includes eight production wells including B06, B07, B16, B18, B26, B27, B29, and B39, as well as four injection wells including B17, B28, B31, and B32. Its main production layers are E2s3U (Upper Member of Shahejie Formation, Neogene Eocene) II + III + IV + V and E2s3M (Middle Member of Shahejie Formation, Neogene Eocene) I Upper + I Lower + II oil formations (Figure 16).

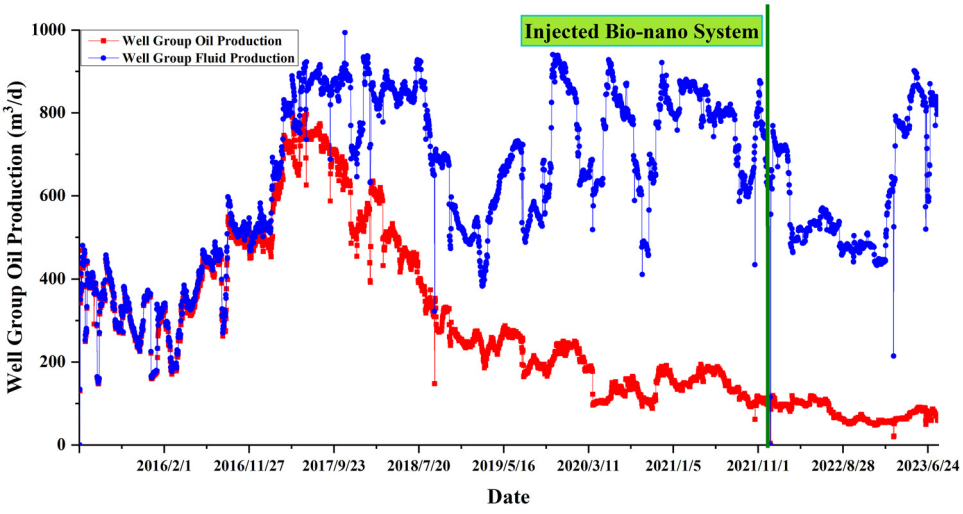

Figure 16: Oil and liquid production of well group.

In the initial phase of block development, there was a rapid decline in oil and liquid production, prompting the commencement of water injection in November 2015. This led to a certain increase in daily oil production. Subsequently, water injection wells were added, and measures such as profile control and water plugging were implemented, resulting in a significant rise in daily oil production while maintaining the water cut at approximately 10–20%. By June 2017, oil production had peaked at 853 m^3; however, it then began to rapidly decrease alongside an escalating water cut. Despite repeated attempts at profile control and managing the water cut, oil production continued to decline rapidly while the water cut increased sharply. By July 2019, the water cut had exceeded 60%, marking entry into a high-water-cut period for oil production. Following several rounds of profile control and adjustments to injection volume, the rate of decline in oil production slowed down. As of October 2021, cumulative block oil production stands at 918,993 m^3 with a recovery factor of 16.54%. Daily oil production is recorded at 145.85 m^3 with a daily fluid volume of 670.96 m^3 and a decline rate of 0.4738 a^{-1}; meanwhile, the water content has reached as high as 78.26%.

Based on the actual production data of the well group (April 2015 to June 2023), the oil production curve and natural decline curve of the well group are drawn, as shown in Figure 17. From the graph, it can be seen that the decrease in oil production of the entire well group occurred after April 2018.

Based on the actual injection and production data of the well group, calculate the increase in oil production according to the production decline formula:

Calculation of oil increment:

$$\Delta Q = \sum_{i=t_0}^{t} Q_i - \int_{t_0}^{t} Q\mathrm{d}t, \tag{24}$$

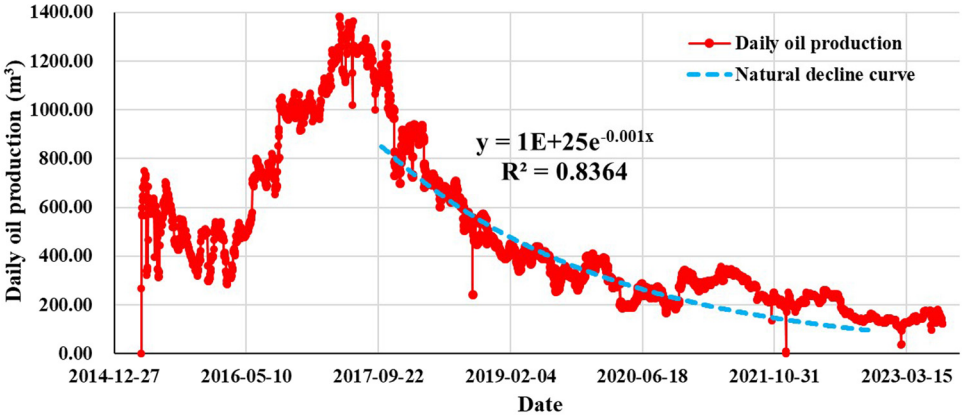

Figure 17: Production performance curve and production decline curve of the well group.

where

$$Q = A \ln(t) + B. \quad (25)$$

In the formula, t_0 is the number of days from the start of production decline when injecting the biological nanocomposite system, Q_i is the actual daily oil production, and A and B are fitting parameters, which are obtained through the decline curve. According to calculations, as of October 2023, the cumulative increase in oil production of the well group is 10253.6 m^3.

Then, using the numerical simulation method proposed in this article, the oil production situation after biological nano oil displacement measures is evaluated. The geological model established in the target block is a single porous medium, which is vertically divided into 246 layers, with a grid size of 1 m for each layer and 63 × 53 grids in the xy plane. Each grid has a length of 25 m, with a total of 821,394 grids. The distribution of well locations is shown in Figure 18.

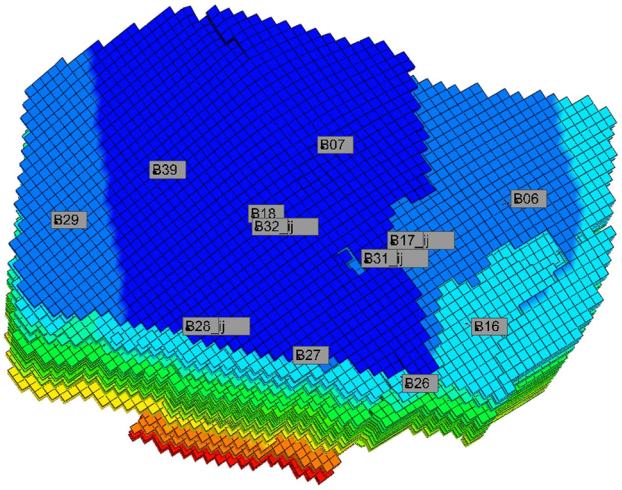

Figure 18: Distribution of well positions in Block B1.

First, the black oil model of the block was converted into the CMG-STARS component model. The numerical simulation method of oil displacement in the biological nanocomposite system is the same as previously and will not be described again here. For an actual oil reservoir, historical fitting is the basis for accurate reservoir dynamic simulation. Therefore, in order to accurately study the oil recovery process of the biological nanocomposite system, water flooding history matching is now performed on the target research block. The fitting of the water content and daily oil production of the well group is shown in Figures 19 and 20, with a fitting degree exceeding 90%, meeting the accuracy requirements.

The simulation began in October 2021 with a reservoir water cut of 79%, injecting the biological nanocomposite system at an injection rate of 1.75 × 10^{-2} and a concentration of 7,000 ppm. As can be seen from the cumulative oil production comparison chart in Figure 21, the rate of cumulative oil production increase after the injection of the biological nanocomposite system has consistently been higher than that without the injection of the biological nanocomposite system. By the end of the simulation period in October 2023, the injection of the biological nanocomposite system had resulted in an additional oil recovery of 10468.92 m^3, demonstrating a significant application effect. The numerical simulation results are in close agreement with the calculations obtained from reservoir engineering methods.

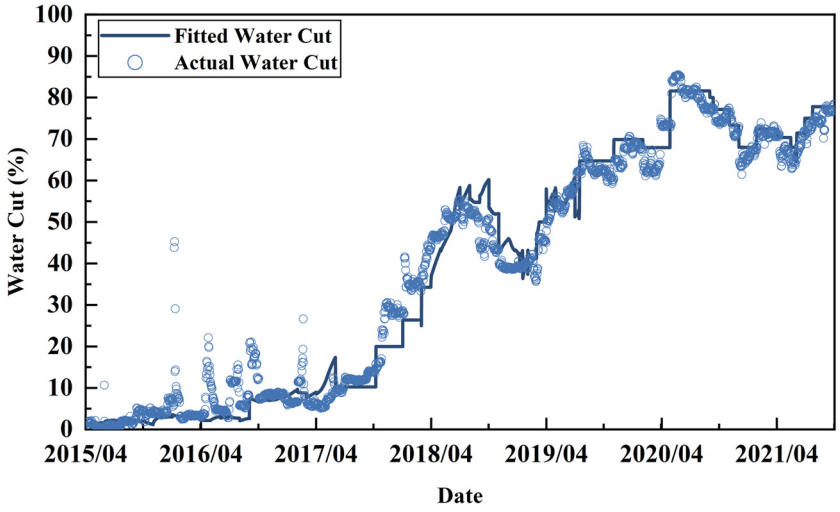

Figure 19: Comparison of actual water content and fitting water content in the block.

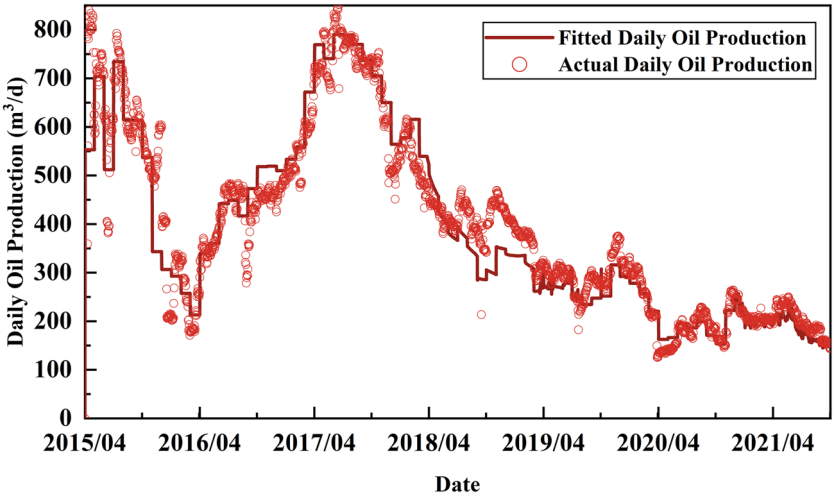

Figure 20: Comparison between actual daily oil production and fitted daily oil production in the block.

5 Discussion

Based on experiments, this study investigated the stability of the biological nanocomposite system and the effects on rock wettability and oil–water interfacial tension. The results indicate that the biological nanocomposite system maintains stable and uniform dispersion after prolonged shear stirring. The measurement results of the wetting angle indicate that the system can shift the wettability of rocks toward hydrophilicity. In addition, the biological nanocomposite system will improve the wettability of sandstone reservoirs better than carbonate reservoirs, due to the interaction between the rock surface and modified nanoparticles. The interface tension test results show that the biological nanocomposite system can reduce the oil–water interface tension to the order of 10^{-3}, which significantly increases the capillary number and makes it easier for crude oil to peel off rocks, significantly improving the flow rate of remaining oil in the reservoir. In summary, the experiment explores the oil displacement mechanism from the perspective of the effect of the biological nanocomposite system on reservoir rocks and fluid properties, and the results are consistent with previous research. Related studies have also shown that temperature, mineralization degree, and pH value can affect the stability of nanofluids. At appropriate temperature, mineralization degree, and pH value, nanoparticles maintain an equilibrium of intermolecular forces in the dispersed system. Once the range is exceeded, nanoparticles will undergo coalescence, leading to a decrease in the performance of the oil recovery system.

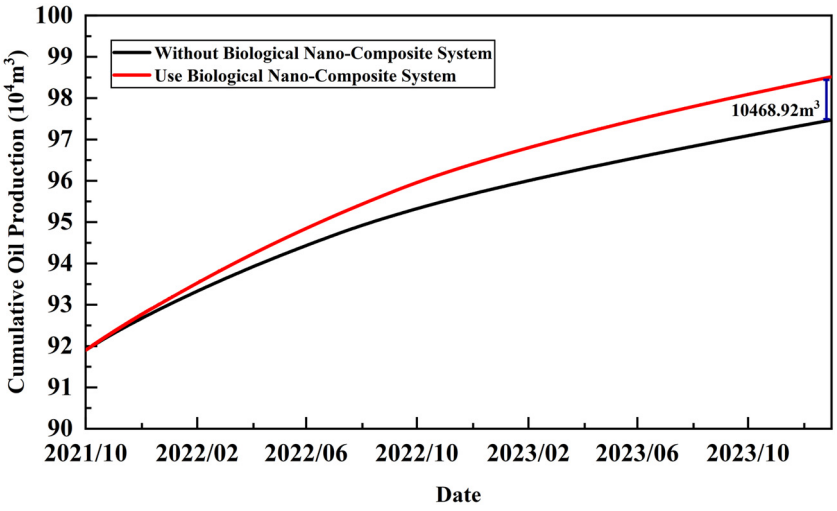

Figure 21: Numerical simulation of cumulative oil production prediction.

However, this article did not consider the influence of these factors on the performance of nanoparticles in the composite system, Future research can consider relevant factors to further improve the performance of the biological nanocomposite system and expand their application scope in fields.

On the basis of indoor experiments, this study established a numerical simulation method for oil recovery using biological nanocomposite system at the reservoir scale. According to research, previous simulation studies on nanofluid flooding have not reached the reservoir scale. The numerical simulation method considers the changes in reservoir wettability and oil–water interfacial tension caused by biological nanocomposite system. This is combined with an improved Brooks Corey model to establish a relative permeability model. At the same time, a numerical characterization method for the transport and adsorption of nanoparticles is added, which can describe the transformation process of reservoir and fluid properties after the biological nanocomposite system is injected underground. Subsequently, the numerical simulation method was validated through core displacement experiments, and the simulation results were highly consistent with the experiments, verifying the accuracy of the model. The components of the displacement system were simplified in the model. In fact, modified nanoparticles not only change the wettability and interfacial tension in the formation, but also improve the overall rheological properties when combined with other oil displacement systems (such as polymers). After injection into the formation, the modified nanoparticles also undergo coalescence, and the charge and polarity of the nanoparticles also have a certain impact on their adsorption. However, the influence of factors such as coalescence, charge, and polarity was not considered in this article. In the future, the above mechanisms can be considered to improve the simulation method of nanoparticle migration in the reservoir.

Subsequently, the multiphase and multi-component model of the biological nanocomposite system for oil recovery was applied to the injection parameters of actual well groups. Unlike other optimization methods, this article comprehensively optimizes the injection amount and concentration of the biological nanocomposite system from two aspects: economic indicators and oil increase. The optimization results were applied to actual mines, and the oil increment was calculated using reservoir engineering methods and numerical simulation methods. The results of the two methods were close, further verifying the accuracy of the numerical method for oil recovery using the biological nanocomposite system. Although the model can evaluate the application effect of biological nanocomposite systems in actual mines, there are still some shortcomings that need further research and development in the future. In the process of optimizing injection parameters using numerical simulation methods, only the injection of a single plug in the biological nanocomposite system was considered. However, in actual field use, other chemical agent plugs are often used in combination, such as a combination of pressure-reducing and injection-increasing plugs, profile control plugs, and nano oil displacement plugs. Pressure-reducing and injection-increasing plugs can remove contamination near the wellbore, improve reservoir connectivity, thereby reducing injection pressure and improving injection performance. Profile control can improve the water absorption profile and increase the coverage range of the injection system. Finally, a nano oil displacement plug is injected to replace the remaining oil. The combination of the three types of plugs can significantly improve the oil displacement efficiency and maximize the oil displacement effect of the system. Therefore, it is necessary to further optimize the slug design based on practical application situations.

This article studies the performance of biological nanocomposite systems through experiments and establishes a multiphase and multi-component oil displacement model based on this. Finally, the injection parameters are optimized and applied to actual mines. However, there are still some shortcomings, and it is necessary to explore the applicability of biological nanocomposite systems in complex geological environments. Numerical simulation methods can also consider more factors for optimization. When optimizing process parameters, it is necessary to consider the combination of slugs based on the actual situation on site. With the increasing demand for oil, biological nanocomposite systems have broad prospects in expanding the affected volume and improving crude oil recovery compared to conventional chemical flooding systems in the future.

6 Conclusions

This article takes the biological nanocomposite system as the research object and conducts research on its oil displacement mechanism, numerical simulation methods, and process parameter optimization methods. The following understanding has been obtained:

1) The biological nanocomposite system, as a system composed of modified nanoparticles and surfactants, can effectively change the wettability of reservoir rocks, reduce the interfacial tension between oil and water,

thereby improving the fluidity of crude oil and increasing the recovery rate;

2) According to the numerical simulation model of the biological nanocomposite system for oil recovery, the injection timing, number of injected PVs, and injection concentration were analyzed. The results indicate that the earlier the biological nanocomposite system is injected, the better its oil-increasing effect. At the same time, due to the limited amount of nanoparticle adsorption, there is an optimal value between the injected PV and the injected concentration. Beyond this value, the economic value of improving the oil enhancement effect brought by the injected PV and injected concentration also decreases;
3) Actual field applications have shown that the biological nanocomposite system can effectively improve reservoir recovery, and the numerical simulation method established in this article can accurately describe the oil displacement performance, with small errors between the calculated results and the actual situation.

In summary, this article provides an effective method for numerical simulation of the biological nanocomposite system for oil recovery and has important guiding significance for the optimization design of process schemes. The biological nanocomposite system has significant potential in improving crude oil recovery.

Funding information: This study was supported by the National Natural Science Foundation of China (Nos 51774257 and 51504221) and the National Science and Technology Major Oil and Gas Special Project (No. 2017ZX05009-004).

Author contributions: Xianchao Chen is responsible for the design and management of the entire study; Jingchao Zhou is responsible for the establishment of mathematical models and the writing of articles; Ping Gao is responsible for numerical simulation to optimize the injection parameters and field applications of biological nanocomposite system. Peijun Liu was responsible for data processing of numerical simulation results and assisted in writing articles; and Qing Feng is responsible for the preparation of the biological nanocomposite system. All authors have accepted responsibility for the entire content of this manuscript and approved its submission.

Conflict of interest: The authors state no conflict of interest.

Data availability statement: The datasets generated during and/or analyzed during the current study are available from the corresponding author on reasonable request.

References

[1] Panchal H, Patel H, Patel J, Shah M. A systematic review on nanotechnology in enhanced oil recovery. Pet Res. 2021;6(3):204–12. doi: 10.1016/j.ptlrs.2021.03.003.
[2] Tackie-Otoo BN, Mohammed MAA, Yekeen N, Negash BM. Alternative chemical agents for alkalis, surfactants and polymers for enhanced oil recovery: Research trend and prospects. J Pet Sci Eng. 2020;187:106828. doi: 10.1016/j.petrol.2019.106828.
[3] Paiaman AM, Al-anazi BD. Feasibility of decreasing pipe sticking probability using nanoparticles. Nafta. 2009;60(12):645–7.
[4] Apteka JW, Cassidy MC, Johnson AC, Barton RA, Lee M, Ogier AC, et al. Silicon nanoparticles as hyperpolarized magnetic resonance imaging agents. ACS Nano. 2009;3(12):4003–8. doi: 10.1021/nn900996p.
[5] Eltoum H, Yang Y, Hou J. The effect of nanoparticles on reservoir wettability alteration: A critical review. Pet Sci. 2021;18(1):136–53. doi: 10.1007/s12182-020-00496-0.
[6] Onyekonwu MO, Ogolo NA. Investigating the use of nanoparticles in enhancing oil recovery. Nigeria Annual International Conference and Exhibition. OnePetro; 2010. doi: 10.2118/140744-MS.
[7] Tola S, Sasaki K, Suai Y. Wettability alteration of sandstone with zinc oxide nano-particles. The 23rd Formation Evaluation Symposium of Japan. OnePetro; 2017.
[8] Li S, Torsæter O. The impact of nanoparticles adsorption and transport on wettability alteration of water wet berea sandstone. SPE Middle East Unconventional Resources Conference and Exhibition. OnePetro; 2015. doi: 10.2118/SPE-172943-MS.
[9] Li S, Dan D, Lau HC, Hadia NJ, Torsæte, Stubbs LP. Investigation of wettability alteration by silica nanoparticles through advanced surface-wetting visualization techniques. SPE Annual Technical Conference and Exhibition. OnePetro; 2019. doi: 10.2118/196192-MS.
[10] Afekare D. Enhancing oil recovery using aqueous dispersions of silicon dioxide nanoparticles: The search for nanoscale wettability alteration mechanism. SPE Annual Technical Conference and Exhibition. OnePetro; 2020. doi: 10.2118/204259-STU.
[11] Cheraghian G, Hendraningrat L. A review on applications of nanotechnology in the enhanced oilrecovery part A: Effects of nanoparticles on interfacial tension. Int Nano Lett. 2016;6(2):129–38. doi: 10.1007/s40089-015-0173-4.
[12] Deng X, Tariq Z, Murtaza M, Patil S, Mahmoud M, Kamal MS. Relative contribution of wettability Alteration and interfacial tension reduction in EOR: A critical review. J Mol Liq. 2021;325:115175. doi: 10.1016/j.molliq.2020.115175.
[13] Wasan DT, Nikolov AD. Spreading of nanofluids on solids. Nature. 2003;423(6936):156–9. doi: 10.1038/nature01591.
[14] Wasan D, Nikolov A, Kondiparty K. The wetting and spreading of nanofluids on solids: Role of the structural disjoining pressure. Curr Opin Colloid Interface Sci. 2011;16(4):344–9. doi: 10.1016/j.cocis.2011.02.001.
[15] Qin W, Zhang Z, Hou B, Yang J. Advance of nanotechnology application in enhancing oil recovery. Fault-block Oil Gas Field. 2013;20(1):10–3. doi: 10.6056/dkyqt201301003.
[16] Ahmed A, Saaid IM, Tunio AH, Pilus RM, Mumtaz M, Ahmad I. Investigation of dispersion stability and IFT reduction using surface modified nanoparticle: enhanced oil recovery. Appl Environ Biol. 2017;7(4S):56–62.
[17] Lim S, Zhang H, Wu P, Nikolov A, Wasan D. The dynamic spreading of nanofluids on solid surfaces-Role of the nanofilm structural

disjoining pressure. J Colloid Interface Sci. 2016;470:22–30. doi: 10.1016/j.jcis.2016.02.044.
[18] Wu W, Hou J, Qu M, Wen Y, Liang T, Yang J, et al. Microscopic flooding mechanism experiment visualization of 2-D smart black nano-card. Oilfield Chem. 2020;37(1):133–7. doi: 10.19346/j.cnki.1000-4092.2020.01.023.
[19] Song R, Wang Y, Liu JJ. Microscopic pore structure characterization and fluids transport visualization of reservoir rock. J Southwest Pet Univ Sci Technol Ed. 2018;40(06):85–105.
[20] Su J, Wang L, Gu Z, Zhang Y, Chen C. Advances in pore-scale simulation of oil reservoirs. Energies. 2018;11(5):1132. doi: 10.3390/en11051132.
[21] Al-Yaari A, Ching DLC, Sakidin H, Muthuvalu MS, Zafar M, Alyousifi Y, et al. Optimum volume fraction and inlet temperature of an ideal nanoparticle for enhanced oil recovery by nanofluid flooding in a porous medium. Processes. 2023;11(2):401. doi: 10.3390/pr11020401.
[22] Liu R, Gao S, Peng Q, Pu W, Shi P, He Y, et al. Experimental and molecular dynamic studies of amphiphilic graphene oxide for promising nanofluid flooding. Fuel. 2022;330:125567. doi: 10.1016/j.fuel.2022.125567.
[23] Guzei DV, Minakov AV, Pryazhnikov MI, Ivanova SV. Numerical investigation of enhanced oil recovery from various rocks by nanosuspensions flooding. J Appl Comput Mech. 2022;8(1):306–18.
[24] Esfe MH, Esfandeh S, Hosseinizadeh E. Nanofluid flooding for enhanced oil recovery in a heterogeneous two dimensional anticline geometry. Int Commun Heat Mass Transf. 2020;118:104810. doi: 10.1016/j.icheatmasstransfer.2020.104810.
[25] Long Q, You Q, Wang K, Zhou B, Jiao H, Yao X, et al. Mechanism and influencing factors of enhanced oil recovery for active SiDots nanofluid assisted fracturing-drainage in low permeability reservoirs: An experimental and numerical simulation study. Geoenergy Sci Eng. 2023;222:211394. doi: 10.1016/j.geoen.2022.211394.
[26] Luo J, Yang H, Xiao P, Wang P, Zheng L, Wang G, et al. Nanofluid flooding technology: theory and practice. Oilfield Chem. 2020;5(4):669–74. doi: 10.19346/j.carolcarrollnki.1000-4092.2020.04.018.
[27] Yu H, Deng X, Liu Y, He Y. Research of nanofluids suitable for imbibition and oil displacement in tight oil reservoirs. Fault-Block Oil Gas Field. 2022;29(5):604–8. doi: 10.6056/dkyqt202205005.
[28] Qu M, Liang T, Hou J, Liu Z, Yang E, Liu X. Laboratory study and field application of amphiphilic molybdenum disulfide nanosheets for enhanced oil recovery. Pet Sci Eng. 2022;208(4):109695. doi: 10.1016/j.petrol.2021.109695.
[29] Liang T, Hou J, Qu M, Zhang W, Wu W. 2-D smart nanocard nanofluid laboratory evaluation and field application in fractured-vuggy carbonate reservoirs. Pet Sci Bull. 2020;5(03):402–11. doi: 10.3969/j.issn.2096-1693.2020.03.034.
[30] Li H, Li X, Zheng J, Xu G, Jia Y, Zhang T. Research and application of nano-flooding technology in Penglai 19-3 oilfield. Petrochem Ind Appl. 2020;39(8):4–8. doi: 10.3969/j.issn.1673-5285.2020.08.002.
[31] Wang B, Deng S, Feng Q, She Y, Zhang F. Preparation and performance evaluation of biological nano-oil displacement agent system. Oilfield Chem. 2023;40(4):677–83. doi: 10.19346/j.cnki.1000-4092.2023.04.017.
[32] Janaghi P, Amani H, Naseri A, Kariminezhad H. Accurate prediction of enhanced oil recovery from carbonate reservoir through smart injection of nanoparticle and biosurfactant. J Pet Sci Eng. 2022;216:110772.
[33] Elakkiya VT, SureshKumar P, Alharbi NS, Kadaikunnan S, Khaled JM, Govindarajan M. Swift production of rhamnolipid biosurfactant, biopolymer and synthesis of biosurfactant-wrapped silver nanoparticles and its enhanced oil recovery. Saudi J Biol Sci. 2020;27(7):1892–9.
[34] Behdadfar MH, Sheng JJ, Esmaeilnezhad E. Designing effective enhanced oil recovery fluid: Combination of graphene oxide, D118 SuperPusher, and Chuback surfactant. J Mol Liq. 2023;390:123081.
[35] Manshad AK, Kabipour A, Mohammadian E, Yan L, Ali JA, Iglauer S, et al. Application of a novel green nano polymer for chemical EOR purposes in sandstone reservoirs: Synergetic effects of different fluid/fluid and rock/fluid interacting mechanisms. ACS Omega. 2023;8(46):43930–54.
[36] Manshad AK, Mobaraki M, Ali JA, Akbari M, Abdulrahman AF, Jaf PT, et al. Performance evaluation of the green surfactant-treated nanofluid in enhanced oil recovery: Dill-hop extracts and SiO_2/bentonite nanocomposites. Energy Fuels. 2024;38(3):1799–812.
[37] Motraghi F, Manshad AK, Akbari M, Ali JA, Sajadi SM, Iglauer S, et al. Interfacial tension reduction of hybrid crude-oil/mutual-solvent systems under the influence of water salinity, temperature and green SiO2/KCl/Xanthan nanocomposites. Fuel. 2023;340:127464.
[38] Ahmad F, Ashraf N, Ashraf T, Zhou RB, Yin DC. Biological synthesis of metallic nanoparticles (MNPs) by plants and microbes: their cellular uptake, biocompatibility, and biomedical applications. Appl Microbiol Biotechnol. 2019;103:2913–35.
[39] Zeth K, Hoiczyk E, Okuda M. Ferroxidase-mediated iron oxide biomineralization: novel pathways to multifunctional nanoparticles. Trends Biochem Sci. 2016;41:190–203.
[40] Varma RS. Greener approach to nanomaterials and their sustainable applications. Curr Opin Chem Eng. 2012;1:123–8.
[41] Feng Q, Gao P, Chen X, Li J, Zhou J, Qian F, et al. Development and application of well-test model after injection biological nanomaterials. Geofluids. 2022;2022:1–16. doi: 10.1155/2022/9717061.
[42] Feng Q, Zhou J, Li S, Chen X, Sun Y, Zhang X, et al. Research on characterization technology and field test of biological nano-oil displacement in offshore medium- and low-permeability reservoirs. ACS Omega. 2022;7(44):40132–44. doi: 10.1021/acsomega.2c04960.
[43] Gao P, Feng Q, Chen X, Li S, Sun Y, Li J, et al. Numerical simulation and field application of biological nano-technology in the low-and medium-permeability reservoirs of an offshore oilfield. J Pet Explor Prod Technol. 2022;12(12):3275–88. doi: 10.1007/s13202-022-01522-0.
[44] Wang S, Hou B, Zhang F, Fan H, Cai F, Zhang J, et al. Mechanism of synergistically changing the surface wettability of oil-wet sandstone by a novel nano-active fluid. Fine Chem. 2022;39(10):2141–8 + 2160. doi: 10.13550/j.jxhg.20220019.
[45] Jiang JR. A study of silica nanoparticles for enhanced oil recovery. Doctoral dissertation. Palo Alto (CA): Stanford University; 2016.
[46] Lin M, Hua C, Li M. Adjusting reservoir rock surface wettability with salt water. Pet Explor Dev. 2018;45(1):136–44. doi: 10.11698/PED.2018.01.14.
[47] Liang X, Zhou F, Wei W, Liu X, Liang T, Zhao X, et al. Study on wettability of tight oil reservoirs based on pore minerals and fluid distribution. Oil Drill Prod Technol. 2021;43(5):651–7 + 674. doi: 10.13639/j.odpt.2021.05.014.

[48] Feng X. Study on modification of nano TiO_2 for oil displacement and its adaptability in low permeability reservoirs. Beijing: China University of Petroleum; 2019.
[49] Hezave AZ, Dorostkar S, Ayatollahi S, Nabipour M, Hemmateenejad B. Effect of different families (imidazolium and pyridinium) of ionic liquids-based surfactants on interfacial tension of water/crude oil system. Fluid Phase Equilib. 2013;360:139–45. doi: 10.1016/j.fluid.2013.09.025.
[50] Ju B, Dai S, Luan Z, Zhu T, Su X, Qiu X. A study of wettability and permeability change caused by adsorption of nanometer structured polysilicon on the surface of porous media. SPE Asia Pacific Oil and Gas Conference and Exhibition; 2022. doi: 10.2118/77938-MS.
[51] Ju B, Fan T. Experimental study and mathematical model of nanoparticle transport in porous media. Powder Technol. 2009;192(2):195–202.
[52] Liu X, Civan F. Characterization and prediction of formation damage in two-phase flow systems. SPE Production Operations Symposium; 1993. doi: 10.2118/25429-MS.
[53] Sepehri M, Moradi B, Emamzadeh A, Mohammadi AH. Experimental study and numerical modeling for enhancing oil recovery from carbonate reservoirs by nanoparticle flooding. Oil Gas Sci Technol – Rev d'IFP Energ Nouvelles. 2019;74:5. doi: 10.2516/ogst/2018080.
[54] Mohammadi H, Delshad M, Pope GA. Mechanistic modeling of alkaline/surfactant/polymer floods. SPE Reserv Eval Eng. 2009;12(4):518–27. doi: 10.2118/110212-PA.
[55] Ding B, Xiong C, Geng X, Guan B, Pan J, Xu J, et al. Characteristics and EOR mechanisms of nanofluids permeation flooding for tight oil. Pet Explor Dev. 2020;47(4):810–9. doi: 10.1016/S1876-3804(20)60096-9.
[56] Ding L, Wu Q, Zhang L, Guérillot D. Application of fractional flow theory for analytical modeling of surfactant flooding, polymer flooding, and surfactant/polymer flooding for chemical enhanced oil recovery. Water. 2020;12(8):2195. doi: 10.3390/w12082195.